Egr1 Expression Is Induced Following Glatiramer Acetate Immunotherapy in Rodent Models of Glaucoma and Alzheimer's Disease

Sharon Bakalash,[1,2] *Michael Pham,*[2,3] *Yosef Koronyo,*[3] *Brenda C. Salumbides,*[3] *Andrei Kramerov,*[4] *Hillary Seidenberg,*[3] *Dror Berel,*[5] *Keith L. Black,*[3] *and Maya Koronyo-Hamaoui*[3,6]

Purpose. Immunization with glatiramer acetate (GA) alleviates the neuropathology associated with glaucoma and Alzheimer's disease (AD) in rodent models. This research was undertaken to screen for molecular factors underlying GA-induced neuroprotective mechanisms in these models of chronic neurodegeneration.

Methods. Gene expression profiles were analyzed in GA-immunized versus nonimmunized elevated-intraocular pressure (IOP) rat models of glaucoma by using whole genome cDNA microarrays and were further validated by quantitative real-time PCR analysis. A gene, prominently upregulated by GA in elevated IOP retina, was further studied in APP_{SWE}/$PS1_{\Delta E9}$-transgenic (AD-Tg) mice after GA immunization.

Results. Seven days after treatment with GA, numerous genes were regulated in the retinas of rats with elevated IOP. Comprehensive functional classification and DAVID/KEGG enrichment analysis of GA-induced differentially expressed genes revealed annotation terms and pathways involved in neuroprotection, immune responses, cell communication, and regeneration. Specifically, increased mRNA levels of an early growth response *(Egr) 1* gene were evident in GA-immunized retinas with elevated IOP. In AD-Tg mice, a significant increase in hippocampal EGR1 protein levels was also found in response to GA immunization. Nuclear EGR1 in the dentate gyrus colocalized more frequently with doublecortin-positive and Ki67 proliferating neural progenitors in GA-immunized as compared to nonimmunized AD-Tg mice. Further, EGR1 levels were negatively correlated with hippocampal amyloid-β plaque burden.

Conclusions. This study presents global gene expression profiles associated with GA immunization in a glaucoma rat model. Moreover, it identifies EGR1 transcription factor as a potential mediator for GA-induced neuroprotection in both glaucoma and AD. (*Invest Ophthalmol Vis Sci.* 2011;52:9033–9046) DOI: 10.1167/iovs.11-7498

Neurodegenerative diseases, whether acute or chronic, are associated with a self-perpetuating process of degeneration in which emerging toxic compounds are often involved (e.g., exceeding levels of glutamate, nitric oxide, and aggregated proteins).[1–8] In addition, most neurodegenerative conditions share a local inflammatory response that is associated with activation of resident glial cells (microglia, astrocytes, and oligodendrocytes), infiltrating immune cells, and neurons.[9–17] Historically, inflammatory response in the CNS was perceived as malevolent suggesting that immune responses in the CNS should be entirely suppressed.

Recent studies, however, documented certain immune responses that are necessary for CNS well-being, especially for restoring homeostasis after injury. Specifically, it was demonstrated that $CD4^+$ T cells recognizing elevated CNS antigens in disease sites are needed for CNS maintenance, and boosting their levels benefits repair.[18–34] To safely boost T-cell responses to self-antigens without the risk of inducing autoimmune disease, we used glatiramer acetate (GA; also known as copolymer-1, Cop-1, [Copaxone]), a synthetic copolymer that weakly cross-reacts with myelin-derived antigens.[35,36] Immunization with GA in rodent models of glaucoma and Alzheimer's disease (AD) was effective in reducing neuronal loss, limiting levels of neurotoxic molecules (i.e., glutamate excess and amyloid-β [Aβ] peptide accumulation) and cell debris, and in arresting local and detrimental inflammation.[19,30,37–43] In models of spinal cord injury and AD, an increased recruitment of monocyte-derived macrophages after GA immunization was documented. These blood-borne monocytes were directly involved in the clearance of toxic components in the brain and the local regulation of overwhelming inflammation, thereby ameliorating the disease pathology.[26,40,44,45]

The induction of chronically elevated intraocular pressure (IOP) in rats (elevated-IOP rats) resulting in the progressive death of retinal ganglion cell (RGC) and functional optic nerve damage is a well-established model mimicking chronic glaucoma.[37,38,46,47] In elevated-IOP rats, GA immunization was protective in reducing RGC loss and attenuating decline in retinal function.[19,37,48] A similar GA immunization protocol in APP_{SWE} and $PS1_{\Delta E9}$ double-transgenic mice (AD-Tg mice) resulted in reduced cerebral Aβ burden and astrogliosis, enhanced neurotrophic support and hippocampal neurogenesis, and improved learning and memory.[39,40,45] Yet the exact molecular mechanism or mechanisms by which peripheral GA immunization confers its CNS neuroprotection is still largely unknown.

From the [1]Department of Ophthalmology, Schepens Eye Research Institute, Harvard Medical School, Boston, Massachusetts; and the [3]Department of Neurosurgery, Maxine-Dunitz Neurosurgical Institute, [4]Opthalmology Research Laboratory at the Regenerative Medicine Institute, [5]Samuel Oschin Comprehensive Cancer Institute, and the [6]Department of Biomedical Sciences, Cedars-Sinai Medical Center, Los Angeles, California.

[2]These authors contributed equally to the work presented here and should therefore be regarded as equivalent authors.

Supported by the Maurice Marciano Family Foundation.

Submitted for publication March 17, 2011; revised August 19 and September 22, 2011; accepted September 23, 2011.

Disclosure: **S. Bakalash**, None; **M. Pham**, None; **Y. Koronyo**, None; **B.C. Salumbides**, None; **A. Kramerov**, None; **H. Seidenberg**, None; **D. Berel**, None; **K.L. Black**, None; **M. Koronyo-Hamaoui**, None

Corresponding author: Maya Koronyo-Hamaoui, Departments of Neurosurgery and Biomedical Sciences, Cedars-Sinai Medical Center, Los Angeles, CA 90048; koronyom@cshs.org.

Previous studies[49–64] have reported similar pathologic processes in glaucoma and AD, especially those leading to RGC death in glaucoma and to neuronal cell degeneration in AD. The presumably common immunologic pathways shared among neurodegenerative disorders, the wide range of neurodegenerative models that benefit from GA immunization,[19,30,39–42,65] and the recent reports suggesting that blood monocytes benefit CNS repair[40,44,66] prompted us to further search for a common molecular fingerprint of GA-mediated response. To elucidate some of these mechanisms, we screened for global gene expression alterations after beneficial GA immunization in an elevated-IOP model for glaucoma and further evaluated the presence of one dominant change in a mouse model for AD.

Here, using whole genome microarrays analysis, we identified alterations in gene expression profiles associated with immune manipulation of the degenerating tissue. We based our screening on tissue taken from an elevated IOP–induced RGC loss rat model of glaucoma.[37,38] Unlike other models of long term chronic neurodegeneration, in which onset is insidious and phenotype variable, this model has a defined onset with lower diversity, yielding a clearer signal-to-noise response. We found multiple changes in gene expression that are associated with immune activity, scar formation, tissue remodeling, and homeostasis regulation. One of the prominent changes found in the IOP-triggered rat retinas after GA immunization was elevation of the early growth response (*Egr*) 1 gene (also known as *Zif268*, *Krox-24*, *Ngfi-a*, *Tis8*, and *Zenk*). EGR1 is a nuclear transcription factor involved in tissue responses to stress signals and is known to induce downstream genes associated with plasticity and repair, especially after injury. In addition to gene analysis, we determined that nuclear EGR1 protein levels were elevated in the hippocampi of AD-Tg mice receiving GA immunization.

Materials and Methods

Animal Models

IOP-Triggered Rats. Inbred adult male Lewis rats (8 weeks old; average weight, 300 g; $n = 18$) were supplied by the Animal Breeding Center at The Weizmann Institute of Science. The rats were maintained in a light- and temperature-controlled room and were matched for age and weight before each experiment. All experimental animals were handled according to the regulations formulated by the Institutional Animal Care and Use Committee (IACUC) and the ARVO Statement for the Use of Animals in Ophthalmic and Vision Research.

AD Transgenic Mice. Double-transgenic $APP_{SWE}/PS1_{\Delta E9}$ (7 months old, females and males at equal numbers; average weight, 40 g; $n = 14$) mice from the B6C3-Tg strain (stock no. 004462) and their age- and sex-matched nontransgenic littermates ($n = 7$) were purchased from the Jackson Laboratories (Bar Harbor, ME). This mouse model expresses the chimeric mouse/human amyloid precursor protein (with the Swedish double mutations $APP_{K595N, M596L}$) and the mutant human gene presenilin 1 (PS1 with deletion in exon 9) under the prion protein (PrP) promoter directed to CNS tissue. AD-Tg mice and non-Tg wild-type (wt) littermates were genotyped, for the presence of the transgenes by analysis of genomic DNA extracted from tail tip, using DNA extraction kit (Qiagen, Valencia, CA), as previously described.[67] All experiments were approved and conducted according to regulations devised by the Cedars-Sinai Medical Center IACUC.

Induction of Chronically Elevated IOP. Blockage of aqueous outflow causes an increase in IOP, resulting in the death of RGCs: an increase in IOP was induced in rats by argon laser photocoagulation of the episcleral veins and limbal plexus.[38,68–70] Briefly, 18 rats were deeply anesthetized (ketamine hydrochloride 50 mg/kg, xylazine hydrochloride 0.5 mg/kg, injected intramuscularly), and the aqueous outflow from their right eyes was blocked by 80 to 120 applications of blue-green argon laser irradiation. The laser beam, which was directed at 3 of the 4 episcleral veins and at 270° of the limbal plexus, was applied with a power of 1 W for 0.2 seconds, producing a spot size of 100 μm at the episcleral veins and 50 mm at the limbal plexus. At a second laser session 1 week later, the same parameters were used except that the spot size was 100 μm for all applications. This time the laser beam was directed toward all four episcleral veins and at 360° of the limbal plexus.[68]

GA Immunization. In the elevated-IOP rat model, GA (100 μg; high-molecular-weight; Teva Pharmaceutical Industries, Petah Tikva, Israel) in phosphate-buffered saline (PBS) was administered subcutaneously to 8-week-old rats ($n = 6$) on the day of the second laser irradiation. An additional age-matched control group ($n = 6$) was injected with only PBS, and an additional rat group ($n = 6$) served as naive controls. In the $APP_{SWE}/PS1_{\Delta E9}$ AD mouse model, 7-month-old AD-Tg mice ($n = 7$) were subcutaneously injected twice a week for the first 2 weeks and then once a week for a total of 3 months with GA (100 μg) in 1× PBS. Age-matched control groups ($n = 7$ per group) were either AD-Tg mice injected subcutaneously with 1× PBS according to the same regimen or untreated non-Tg naive mice. At the end of the study, all mice were perfused under anesthesia with 1× PBS, and half-hemisphere brain tissues were postfixed in 2.5% paraformaldehyde (Sigma-Aldrich, St. Louis, MO), and the remaining tissues were snap frozen for further protein and RNA analysis.

Gene Expression Analysis

GeneChip Set: Whole Rat Genome Microarrays Analysis. Arrays (Rat Genome 230A+B GeneChip; Affymetrix, Santa Clara, CA) containing 31,100 probe sets representing more than 15,900 well-substantiated rat genes and expressed sequence tags (ESTs; unknown genes) were used. The sequences spotted on this chip were selected from GenBank, dbEST, and RefSeq. Sequence clusters were created from the UniGene database (Build 99, June 2002) and were refined by analysis and comparison with other publicly available draft assemblies of the rat genome from the Baylor College of Medicine Human Genome Sequence Center (June 2002). For further details, see http://www.affymetrix.com.

Sample Preparation and Hybridization. In the elevated-IOP rat model, three groups, each comprising six rats as described, were used to study global alterations in gene expression. The right (elevated-IOP) retina of each rat was dissected out under RNase-free conditions, and total retinal RNA was extracted using reagent (TRIzol; Invitrogen, Carlsbad, CA). Three retinal RNA samples from each experimental group (IOP-GA, IOP-PBS, naive) were randomly pooled together into a single specimen and then applied onto two independent hybridization (GeneChip; Affymetrix) kits. Pooling identical quantities from several RNA samples into one specimen and performing multiple repetitions on the Affymetrix plate allowed for a high validity index. RNA was isolated (RNeasy Mini Kit; Qiagen) and converted to double-stranded cDNA (Gibco BRL Superscript Choice System; Life Technologies, Rockville, MD) and then to biotinylated cRNA (Bioarray High-Yield RNA Transcription Labeling Kit; Enzo Diagnostics, Farmingdale, NY), according to the manufacturers' protocols. After fragmentation and quality confirmation with another array (Test3; Affymetrix), the biotinylated cRNA was hybridized (Rat Genome 230A+B GeneChip; Affymetrix). Hybridized chips were washed, stained with streptavidin-phycoerythrin, and scanned with a probe array scanner.

In the AD mouse model, RNA extraction and isolation were performed immediately after brain collection. Whole forebrain tissues from non-Tg (wt) and AD-Tg mice (GA immunized and PBS treated) were placed in reagent (TRIzol; Invitrogen) and snap frozen for processing at a later time. For RNA extraction, tissue was quickly thawed and homogenized in reagent (TRIzol) according to manufacturer's protocol (Life Technologies, Invitrogen). At the last step, to eliminate genomic DNA contamination, the upper aqueous phase containing RNA was passed through a spin column (gDNA Eliminator; Qiagen) and

RNA was isolated (RNeasy kit; Qiagen) according to the manufacturer's instructions.

Microarray Data Analysis and Statistics. Probe signal summation, normalization, and background subtraction were performed by a robust multi-array averaging (RMA) method[71] using the affy package from Bioconductor.[72] Differentially expressed genes were selected by calculating their statistical significance using the Linear Models in a Microarray (LIMMA) package. This package allowed us to improve the variance estimation of duplicates using an empirical Bayesian method.[73] Because genes were represented in the arrays in more than one spot (triplicates), we avoided false-positive results by verifying a consistent differential expression in all the spots. Differentially expressed GA-induced genes were defined as significant, with $P < 0.05$ and ≥1.3-fold change. Functional categorization and classification of GA-induced differentially expressed genes was performed according to functional annotation data, including the Gene Ontology and KEGG pathway (Kyoto Encyclopedia of Genes and Genomes), based on gene set enrichment analysis using the online tools DAVID (Database for Annotation, Visualization and Integrated Discovery).[74,75]

Quantitative Real-Time PCR. Total RNA purification from rat retinas was performed as described. For cDNA synthesis, we used 1 to 2 μg total DNase I–treated RNA from each sample that were dilute-adjusted with sterile DDW to the reaction concentration. Reverse transcription into cDNA was performed as follows: RNA dilutions were heat-denatured at 70°C for 10 minutes, chilled on ice, and mixed with cDNA reaction mix containing murine reverse transcriptase enzyme (SuperScript RT; Invitrogen), buffer (SuperScript RT Buffer; Invitrogen), inhibitor (RNase Inhibitor; Invitrogen), dNTP mix, dithiothreitol, and oligo dT primers. This was followed by incubation at 42°C for 50 minutes and at 70°C for 15 minutes. The double-stranded cDNA was stored in −20°C until use for PCR reactions. Several differentially expressed genes and two reference genes were chosen for assaying the relative expression of mRNA levels by fluorescence-based real-time PCR to verify microarray data. These genes were selected based on their relevance to CNS neurodegeneration or neuroprotection and their microarray expression alterations of >1.3-fold. For the real-time PCR, we used the original (unpooled) cDNA of each animal from all matched experimental groups in the presence of gene-specific primers constructed according to exon-exon junctions. The primers (Supplementary Table S4, http://www.iovs.org/lookup/suppl/doi:10.1167/iovs.11-7498/-/DCSupplemental) were designed using Primer 3 Web free software and were directed to mRNA-originated DNA populations while excluding genomic DNA by designing primers to the exon junctional areas and excluding repetitive sequences. BLAST searches were performed to confirm the gene specificity of each primer.

Genes were successfully calibrated to the quantitative real-time PCR analyses to obtain optimal efficiencies of PCR reaction kinetics (Rotor-Gene 6 instrument; Corbett Research, Sydney, Australia) and were analyzed with (Rotor-Gene 6000 software; version 1.7; Corbett). Reactions were calibrated to obtain standard curves with efficiency values close to 1.00 (±0.02), by means of optimizing primer dilutions for each primer set. Melting curves for each primer set (gene) were also evaluated for reaction specificity. All real-time reactions were carried out under the same amplification conditions: 95°C for 5 seconds, 60°C for 20 seconds, and 72°C for 15 seconds, for 40 cycles. Reactions were performed with a mix (AbsoluteQPCR SYBR Green ROX; ABgene, Portsmouth, NH) containing DNA polymerase (Thermostart; Portsmouth), dNTPs, MgCl2, SYBR Green I dye, and ROX reference dye. Products were detected by the SYBR Green I dye detector absorbed at 519 nm, obtained in triplicate for each of the cDNA samples. We used mean cycle threshold (Ct) values to compare relative quantities between experimental groups. Relative mRNA amounts were evaluated by the relative standard curve method ($2^{\Delta\Delta Ct}$),[76] assuming similar PCR efficiencies of the gene of interest relative to an endogenous reference gene. Glyceraldehyde 3-phosphate dehydrogenase (*Gapdh*) and cytoplasmic β-Actin were chosen as reference genes. Real-time PCR reactions for genes of interest and for endogenous controls were always performed on the same reaction plate.

For the evaluation of *Egr1* mRNA levels in the AD mouse model, 2 μg total RNA was used for reverse transcription using a cDNA synthesis kit (iScript; Bio-Rad, Hercules, CA). Quantitative real-time PCR analysis was carried out (Rotor Gene 6000 and Rotor-Gene SYBR Green PCR kit; Qiagen). The average threshold cycle for each gene was determined from triplicate reactions, and the expression level was normalized to *Gapdh*. Primers were designed using Primer 3 Web free software, constructed according to exon-exon junctions (as described) and were synthesized and purchased from Invitrogen (Supplementary Table S4, http://www.iovs.org/lookup/suppl/doi:10.1167/iovs.11-7498/-/DCSupplemental). Cycling conditions were 95°C for 10 seconds, 60°C for 10 seconds, and 72°C for 20 seconds.

Protein Analysis

Immunohistochemistry. Brain cryosections (30-μm thick) isolated from AD-Tg and non-Tg mice were treated with a permeabilization/blocking solution containing 20% horse serum (Invitrogen) and 0.01–0.1% Triton X-100 (Sigma-Aldrich). Sections were stained overnight at 4°C with a specific combination of the following primary mAbs in PBS containing 10% blocking solution: mouse anti–mouse EGR1 (1:350; AB54966; Abcam, Cambridge, MA), rabbit anti–mouse Ki67 (1:100; AB15580; Abcam), mouse anti–human Aβ (residues 17–24, clone 4G8 [1:100; SIG-39,220; Covance]), and goat anti–mouse double cortin (DCX; 1:100; SC-8066; Santa Cruz Biotechnology, Santa Cruz, CA). Next, sections were incubated for 1 hour at room temperature with secondary antibodies and washed three times with PBS; then and a mounting solution (Vectashield; Vector Laboratories, Burlingame, CA) with or without 4′, 6-diamidino-2-phenylindole dihydrochloride (DAPI; Vector Laboratories) was applied. Secondary antibody solution was applied in 1× PBS and consisted of Cy3- and Cy2-conjugated donkey anti–mouse, anti–goat, and/or anti–rabbit antibodies (1:200; Jackson ImmunoResearch Laboratories, West Grove, PA), depending on the combination of primary antibodies used. Additionally, EGR1 immunoreactivity was visualized by the nonfluorescence immunoperoxidase method using 3,3′-diaminobenzidine as the chromogen (DAB substrate; Sigma-Aldrich) and an ABC kit (Vectastain; Vector Laboratories) as specified by the manufacturer. Routine controls were processed using the same protocol with the omission of the primary antibody.

Microscopy. Fluorescence and bright-field images were acquired using a fluorescence microscope (Axio Imager Z1; Carl Zeiss MicroImaging, Inc., Thornwood, NY) equipped with a slider module (ApoTome; Carl Zeiss MicroImaging, Inc.) at the same setting and exposure times for each experiment. For processing and analysis of the images, accompanying software (AxioVision, version 4.6.3; Carl Zeiss MicroImaging, Inc.) was used. Carl Zeiss filter sets were used for excitation/emission at 365/445 nm for DAPI, 470/525 nm for Cy2, and 550/605 nm for Cy3.

Quantitative Immunohistochemical Analysis. Images of stained tissues were obtained on a fluorescence microscope (Axio Imager Z1; Carl Zeiss MicroImaging, Inc.) with a motorized Z-drive and with a monochrome camera (AxioCam MRm, version 3.0 [Carl Zeiss MicroImaging, Inc.], at a resolution of 1388 × 1040 pixels, 6.45 μm × 6.45 μm pixel size, dynamic range >1:2200, that delivers low-noise images because of the Peltier-cooled sensor). Quantitative analysis of the EGR1-positive cell count (stained with DAB as a chromogen) and the 4G8-positive Aβ plaque area in the hippocampus was performed using three coronal sections (two hemispheres each) per mouse at 450-μm intervals, over an area covering the hippocampus. Optical sections from each field of the specimen were imported into ImageJ software (developed by Wayne Rasband, National Institutes of Health, Bethesda, MD; available at http://rsb.info.nih.gov/ij/index.html). Conversion to grayscale was performed to distinguish between areas of immunoreactivity and background. Total area of immunoreactivity was determined using a standardized histogram-based threshold technique.

Cells that were positively labeled with DAB were individually counted using the ImageJ native counter, and average cell counts were compared across all experimental groups.

Western Blot Analysis. Mouse hippocampal nuclear protein lysate was prepared and homogenized in a lysis buffer containing PBS, Triton X-100 0.03% (Sigma-Aldrich), and protease inhibitors 1× (Cocktail set I, Calbiochem). The homogenate was centrifuged at 350*g* for 10 minutes at 4°C to remove the cell debris, and the supernatant was centrifuged again at 1000*g* for 10 minutes at 4°C to render protein fractions for analyses. The pellet fraction containing nuclei were lysed in buffer containing PBS, Triton X-100 0.5% (Sigma-Aldrich), and protease inhibitors. The total protein concentration was determined using a BCA protein assay (Pierce, Rockford, IL). Proteins (34 μg) were mixed with an equal volume of the 2× SDS-sample buffer (Invitrogen) containing 5% β-mercaptoethanol, separated by SDS-electrophoresis on a 4% to 20% Tris-Glycine polyacrylamide gel (Invitrogen), and transferred onto nitrocellulose membranes. After blocking in 5% nonfat milk and 0.05% Tween-20 in PBS, blots were incubated with mouse monoclonal antibodies against total EGR1 (1:200 dilution, Abcam; ab54966) and mouse antibodies against ACTB (1:20,000 dilution; Sigma-Aldrich). For detection, alkaline phosphate–conjugated goat anti–mouse secondary antibodies were used (Jackson ImmunoResearch Laboratories) with BCIP/NBT substrate (Invitrogen). Relative EGR1 protein levels were analyzed and quantified compared with the reference protein (ACTB), using ImageJ software.

Quantitative ELISA. Samples of one brain hemisphere were collected after perfusion. Tissue was homogenized in 4× vol/wt PBS containing protease inhibitor cocktail (Protease Inhibitor Cocktail Set I; Calbiochem, Gibbstown, NJ). Supernatant was collected after centrifugation at 10,000*g* for 15 minutes at 4°C, and the total protein concentration in 1 mL was measured by Bradford assay (Bio-Rad). Levels of soluble human $A\beta_{(1-42)}$ in mouse brain homogenate were determined using a solid-phase sandwich ELISA kit (Invitrogen; precoated plates with rabbit anti–h$A\beta_{(1-42)}$ antibody, that reacts specifically with the human C'-terminal portion of the mature Aβ peptide; no cross-reactivity with the human $A\beta_{(1-40)}$ or $A\beta_{(1-43)}$ or APP), according to the manufacturer's instructions (R&D Systems, Inc., Minneapolis, MN), according to the manufacturer's instructions. The optical density of each well was read at 450 nm (with 540-nm correction) using a microplate reader (Molecular Devices, Sunnyvale, CA).

Statistical Analysis. Means and standard deviations of the obtained data, at both gene expression and protein levels, were calculated for each experiment. Real-time PCR relative quantitative analyses were statistically evaluated using the Student's *t*-test. Microarray statistical analyses were performed as described. One-way analysis of variance (ANOVA) with Bonferroni posttest was used for comparing means of three or more variables. For correlation analysis, a nonparametric Spearman test was applied. Statistical analysis was carried out using graphing and statistics software (Prism [GraphPad, La Jolla, CA] for Macintosh OS X, version 5.0b [Apple, Cupertino, CA] on a Windows XP system [Microsoft, Redmond, WA]rsqb]). The threshold for statistical significance was set at 0.05.

Results

Microarray Analysis of Gene Expression Altered by GA Immunization in Elevated IOP

To identify genes possibly associated with the beneficial effect of GA immunization, we first focused on a model of elevated IOP. We compared global gene expression profiles using cDNA microarray (Affymetrix) of retinal tissues from rats that were subjected to chronically elevated IOP and were treated with either a single GA immunization (IOP-GA; $n = 6$) or vehicle injection (IOP-PBS; $n = 6$). These groups were initially compared with naive control rats ($n = 6$). Only those genes whose expression was significantly altered ($P < 0.05$) compared with the naive retina were further analyzed to identify genes associated with GA immunization. This analysis of IOP-GA versus IOP-PBS groups revealed multiple changes in retinal gene expression as a result of GA immunization (244 and 252 transcripts were significantly repressed and induced, respectively; Supplementary Tables S1–S3; http://www.iovs.org/lookup/suppl/doi:10.1167/iovs.11-7498/-/DCSupplemental).

GA-induced differentially expressed genes were further divided into the following three categories: genes that were significantly altered (induced or repressed) as a result of elevated IOP and were restored to their basal levels after GA immunization (67 and 37 transcripts were significantly repressed or induced, respectively, toward the normal levels) (Supplementary Tables S1A, S1B, and Fig. S1, a heat diagram; http://www.iovs.org/lookup/suppl/doi:10.1167/iovs.11-7498/-/DCSupplemental); genes that were significantly altered (repressed or induced) because of elevated IOP and were further altered by GA (8 and 6 transcripts were significantly further repressed and induced, respectively) (Supplementary Table S2, http://www.iovs.org/lookup/suppl/doi:10.1167/iovs.11-7498/-/DCSupplemental); genes that remained unchanged after IOP elevation but were altered as a result of GA (69 and 70 transcripts were significantly repressed and induced, respectively) (Supplementary Tables S3A, S3B, http://www.iovs.org/lookup/suppl/doi:10.1167/iovs.11-7498/-/DCSupplemental).

GA-Induced Neuroprotective Terms and Pathways Identified by Gene Set Analyses

Genes significantly altered in all three categories were ontologically classified based on function and structure (AmiGO; gene ontology, GO consortium). Genes were clustered according to the following biological functions: cell adhesion, extracellular matrix components, cytoskeleton proteins, motility and migration, immune response, development, cell differentiation and proliferation, cell cycle, and cell death. We found that GA immunization in elevated-IOP rats caused a retinal induction of transcripts relevant to tissue maintenance, repair, and renewal (Fig. 1). Pie charts show the relative distribution (%) of clusters of differentially regulated genes induced (Fig. 1A) or repressed (Fig. 1B) 1 week after GA immunization. This analysis demonstrates that GA preferentially repressed genes associated with cell death (threefold more than induced), scar tissue formation (14% repressed vs. 8% induced), and protein degradation-ubiquitination (6% repressed vs. 0% induced), but preferentially induced genes associated with growth and neurogenesis (13% induced vs. 9% repressed), development, migration and, differentiation (15% induced vs. 8% repressed), and transcription regulation (14% induced vs. 5% repressed).

Furthermore, differentially expressed genes in response to GA underwent generic set enrichment analysis using DAVID, a multisource (e.g., GO and KEGG) functional annotation data mining tool. Table 1 presents the 25 most significant GA-induced DAVID-enriched annotation terms consisting of 17 statistically significant terms ($P < 0.05$), including a significant aminoacyl-tRNA biosynthesis pathway ($P = 0.009$) revealed by KEGG analysis. Other pathways identified by enrichment analysis of KEGG include networks and molecular interactions involved in cell cycle and cancer, neurotrophic support, neuroactivity, and immune responses but did not reach statistical significance (Supplementary Table S5, http://www.iovs.org/lookup/suppl/doi:10.1167/iovs.11-7498/-/DCSupplemental). Table 2 highlights specific GA-induced enriched terms with neuroprotective-related genes, revealing their functional relevance to processes such as cell migration, proliferation and communication, immune system response and development, extracellular matrix formation, synaptic transmission, and transcription regulation. Subsequently, certain genes (Table 2) were selected for further investigation.

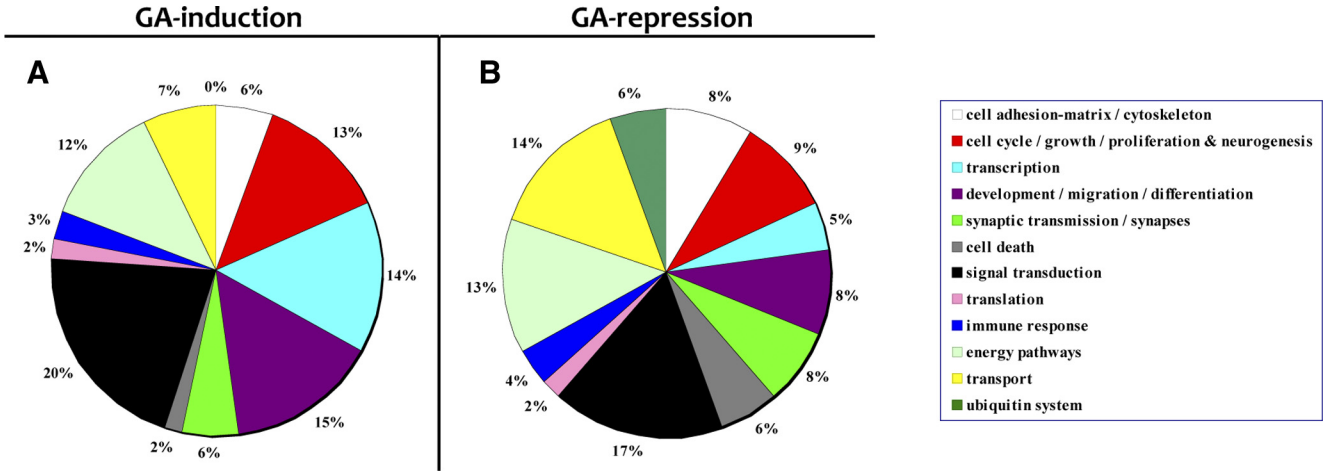

Figure 1. Analyses of gene ontology clusters of significantly altered genes in retinas from elevated IOP rats after GA immunization. Analysis indicates change mostly in genes related to cell death or proliferation, differentiation and migration, transcription, ubiquitination, and transport. Pie charts show the distribution (%) of differentially regulated genes (IOP-GA vs. IOP-PBS) classified according to the gene ontological terms for biological function (AmiGO; the GO consortium). (**A**) GA-induced gene clusters and (**B**) GA-repressed gene clusters.

Quantitative Real-Time PCR Validation of Gene Array Results

To validate changes in gene expression greater than 1.3-fold, we used quantitative real-time PCR, making use of the original unpooled cDNAs from five to six matched rats in the presence of gene-specific primers we constructed according to exon-exon junctions and SYBR Green dye detector (Supplementary Table S4, http://www.iovs.org/lookup/suppl/doi:10.1167/iovs.11-7498/-/DCSupplemental). *Gapdh* and *β-Actin* were incorporated into this analysis as reference genes. Table 3 lists average fold/ratio changes in gene expression in comparison between IOP-GA and IOP-PBS groups: six genes that were successfully calibrated to the real-time PCR analyses to obtain efficiencies of PCR-reaction kinetics that are optimal or extremely close to 1.00 (± 0.01) were included. Quantitative PCR demonstrated that the expression levels of mRNA loci transcripts of Chondroitin sulfate proteoglycan *(Cspg) 2,* Fibrillin *(Fbn) 1,* Ectonucleotide pyrophosphatase/phosphodiesterase *(Enpp) 2,* Neural cell adhesion molecule *(Ncam) 1,* Signal transducer and activator of transcription *(Stat) 1,* and Early growth response

Table 1. Top 25 Annotation Clusters Identified by DAVID, Represented by Terms Enriched by the GA-Induced Genes in Elevated IOP Retina

No.	Term ID	Term Name	Count	%	*P*
1	UP_SEQ_FEATURE	Topologic domain: cytoplasmic	45	21.03	<0.0001
2	SP_PIR_KEYWORDS	Glycoprotein	54	25.23	<0.0001
3	GO:0005886	Plasma membrane	59	27.57	0.0001
4	GO:0030335	Positive regulation of cell migration	8	3.74	0.0010
5	GO:0016023	Cytoplasmic membrane-bound vesicle	20	9.35	0.0010
6	GO:0007166	Cell surface receptor linked signal transduction	32	14.95	0.0021
7	UP_SEQ_FEATURE	Fibronectin type III 2	6	2.80	0.0027
8	IPR007110	Immunoglobulinlike	12	5.61	0.0035
9	GO:0044456	Synapse part	12	5.61	0.0055
10	GO:0031012	Extracellular matrix	11	5.14	0.0067
11	KEGG_pathway/rno00970	Aminoacyl-tRNA biosynthesis*	5	2.34	0.0089
12	GO:0035019	Somatic stem cell maintenance	3	1.40	0.0112
13	GO:0030155	Regulation of cell adhesion	7	3.27	0.0204
14	GO:0032553	Ribonucleotide binding	35	16.36	0.0211
15	IPR001881	EGF-like calcium-binding	5	2.34	0.0237
16	GO:0006836	Neurotransmitter transport	6	2.80	0.0276
17	GO:0042462	Eye photoreceptor cell development	3	1.40	0.0473
18	GO:0048008	Platelet-derived growth factor receptor signaling	3	1.40	0.0567
19	GO:0014069	Postsynaptic density	5	2.34	0.0593
20	GO:0048864	Stem cell development	3	1.40	0.0616
21	GO:0030099	Myeloid cell differentiation	5	2.34	0.0627
22	GO:0032583	Regulation of gene-specific transcription	6	2.80	0.0636
23	GO:0010647	Positive regulation of cell communication	10	4.67	0.0946
24	GO:0008284	Positive regulation of cell proliferation	11	5.14	0.1298
25	GO:0051960	Regulation of nervous system development	7	3.27	0.1987

Most significant terms and pathways derived from top enriched clusters of DAVID functional annotation analysis for GA-induced differentially expressed genes in elevated IOP rat retinas. Term is the name of a detailed item in the annotation source and is associated with a unique ID (i.e., gene ontology or pathway name). Terms of similar annotation are grouped together into clusters. Count is the number of GA-induced genes involved in the term. Percentage is the ratio between GA-induced genes and total genes in this term. *P* value is of the modified Fisher exact test. Terms are ordered by *P* value.

* Detailed and complementary KEGG pathway analysis is available in supplementary Table 5.

TABLE 2. GA-Induced Enriched Annotation Terms Selected Based on Functional Relevance to Neuroprotection

Term ID	Term Name	Genes Involved	*P*
SP_PIR_KEY WORDS	Glycoprotein	*Syt1, Kcnc3, Asam, Pdgfa, Tgfb1, Ssr1, Agtr2, Slcs, Il1rap, Il11ra1, Fbxo23, Vwa1, Odz2, Adam10, Bst1 & 2, Scn2b,* ***Ncam1****, Grm3, Htr6, Vegfa, Efna5,* ***Cspg2 (Vcan)****, Ptgfrn, Ptafr, Calcr, Tpst1, Ecel1,* ***Enpp2****, Gpr149, Lgals3bp, Adra2a, Kcne2, Hsd17b7, Gucy2g, Ces3, Rtn4r, Celsr2, Rfng, Sod3, Lamp1, Mgl1, Sned1, Prlr, Nphs1, Ntrk2, Chrne, Lhb*	<0.0001
GO:0030334	Regulation of cell migration	*Spag9, Gtpbp4, Adam10,* ***Enpp2****, Pdgfa, Vegfa, Igf1, Kit, Tpm1, Tgfb1, Akt2*	<0.001
GO:0007166	Cell surface receptor-linked signal transduction	*Calcr, Nog, Ecel1, Plxna2, Pdgfa, Gpr149, Tiparp, Abca1, Kit, Tgfb1, Eif4ebp1, Agtr2, Adra2a, Axin2, Camk2a, Akt2, Adam10, Igf1, Celsr2,* ***Stat1****, Gnat3,* ***Ncam1****, Grm3, Prlr, Gsk3a, Htr6, Vegfa, Ntrk2, Crb, Ptpn1, Lhb, Ptafr*	0.002
IPR007110	Immunoglobulin-like	***Ncam1****, Rt1-A1, Scn2b, Asam, Ntrk2, Nphs1, Il1rap, Il11ra1,* ***Cspg2 (Vcan)****, Rt1-S3, Ptgfrn, Kit*	0.003
GO:0031012	Extracellular matrix	*Fbln1, Lgals3bp,* ***Fbn1****, Vegfa, Col6a2, Igf1,* ***Cspg2 (Vcan)****, Mmp14, Vwa1, Sod3, Tgfb1*	0.007
KEGG_pathway/ rno00970	Aminoacyl-tRNA biosynthesis	*lArs, Yars, Cars, Lars, Mars*	0.009
GO:0035019	Somatic stem cell maintenance, development, and differentiation*	*Nog, Igf1, Kit*	0.011
GO:0045202	Synapse	*Syt1, Dlgap1, Adam10, Lzts1, Lin7c, Vti1a, Grm3, Slc2a3, Rasgrp2, Ntrk2, Adra2a, Camk2a, Chrne*	0.013
GO:0030155	Regulation of cell adhesion	*Gtpbp4, Adam10, Prlr, Celsr2, Mmp14, Tpm1, Tgfb1*	0.02
IPR001881	EGF-like calcium-binding	*Fbln1, Sned1,* ***Fbn1, Cspg2 (Vcan)****, Celsr2*	0.024
GO:0032869	Cellular response to insulin stimulus	*Eif4ebp1, Gsk3a, Ptpn1,* ***Stat1****, Akt2*	0.045
GO:0030099	Myeloid cell differentiation	*Calcr, Alas2, Vegfa, Kit, Tgfb1*	0.063
GO:0010647	Positive regulation of cell communication	***Ncam1****, Bst2, Atp2c1, Ntrk2, Vegfa, Igf1, Kit, Lgals9, Tgfb1, Akt2*	0.095
GO:0008283	Cell proliferation	*Ppp1r8, Pdgfa, Vegfa, Igf1, Kit, Mmp14,* ***Stat1****, Tgfb1*	0.138
GO:0050804	Regulation of synaptic transmission	***Egr1****, Grm3, Lzts1, Ntrk2, Kit, Camk2a*	0.173
GO:0030099	Myeloid cell differentiation	*Calcr, Alas2, Vegfa, Kit, Tgfb1*	0.06
GO:0002520	Immune system development	*Calcr,* ***Egr1****, Alas2, Tiparp, Vegfa, Kit, Tgfb1*	0.28
GO:0007610	Behavior	***Egr1****, Agtr2, Rac2,* ***Enpp2****, Pdgfa, Atg7, Ntrk2, Crb, Igf1, Kit, Ptafr*	0.189
GO:0010033	Response to organic substance	***Egr1****, Adam10, Pdgfa, Slc22a8, Igf1, Asns, Mmp14,* ***Stat1****, Anxa5, Tgfb1, Gnat3, Agtr2, Eif4ebp1, Cdkn1b, Sds, Gsk3a, Col6a2, Ptpn1, Id3, Ptafr, Akt2*	0.195
GO:0030528	Transcription regulator activity	***Egr1****, Erf, Nrbf2, Ldb2, Rorb, Nfix, Phf12,* ***Stat1****, Tgfb1, Taf5l, Gtf2a1, Irf7, Nab2, Id3, Nr2f2*	0.77

Annotation terms and pathways derived from DAVID enrichment analysis selected by most significant *P* values and functional relevance to GA-induced neuroprotection. Shown for each term are the GA-induced differentially expressed genes that are most highly abundant. Bold genes were further investigated and validated by quantitative real-time PCR.

* Enriched cluster also composed of three terms: stem cell maintenance, development, and differentiation (term IDs, 0019827, 0048863, and 0048864; $P = 0.05$, $P = 0.06$, and $P = 0.08$, respectively). *P* value is of the modified Fisher exact test.

(Egr) 1 were reproducible and consistent with the microarray data. Real-time PCR analyses confirmed that quantitative gene expression analyses of these genes strongly correlated with analyses of the GA-induced changes in gene expression arrays. Real-time PCR analysis provided accurate evaluation of the relative mRNA expression levels because these were analyzed for each individual rat rather than as pooled samples (Table 1, Fig. 2). Figure 2 presents the specific contribution of GA immunization on separate gene expression to the degenerating-injured retina relative to the noninjured retina. Importantly, most genes (5 of 6) that were elevated as result of IOP insult were restored close to normal (nonpathologic) values by GA immunization (Fig. 2). *Egr1*, a gene that was unchanged as a result of injury but that was substantially induced by GA immunization, intrigued us as a potential candidate for GA-induced repair mechanisms. Studies have shown the involvement of *Egr1* in tissue plasticity and repair after injury.[77–80] Therefore, we further focused on the involvement of this gene in another neurodegenerative condition benefiting from GA immunization, the AD model.

Induction of Hippocampal EGR1 after GA Immunization in an Alzheimer's Mouse Model

Egr1 expression was reported to be required for synaptic plasticity and memory formation, particularly in brain regions with a high degree of activity-dependent plasticity, such as the hippocampus.[81–84] In the context of AD, *Egr1* was also shown to affect the expression of genes that regulate the formation of the toxic Aβ peptides associated with AD pathology, such as

TABLE 3. Selected Group of Differentially Expressed Genes Revealed by Whole Genome Microarray Analyses for Further Validation by qRT-PCR

Gene Name (Symbol)	Microarray FC	Real-Time FC
Chondroitin sulfate proteoglycan 2 *(Cspg2)*	−1.32	−1.5
Fibrillin 1 *(Fbn1)*	−1.76	−2.24
Ectonucleotide pyrophosphatase/phosphodiesterase 2 *(Enpp2)*	−2.05	−2.7
Neural cell adhesion molecule 1 *(Ncam1)*	−1.37	−1.87
Signal transducer and activator of transcription 1 *(Stat1)*	−1.43	−1.43
Early growth response 1 *(Egr1)*	1.98	2.17

Real-time PCR ratios (fold changes) refer to the relative expression of genes compared with the *Gapdh* reference gene between two experimental groups, IOP-GA and IOP-PBS. Negative numbers represent the change folds of repressed genes. Results were validated twice by real-time PCR and further compared with a *β-Actin* reference gene. Each rat was analyzed separately in triplicates; $n = 6$ rats per group.

PSEN2 (presenilin 2; a member of the γ-secretase complex).[80,85] Weekly GA immunization in AD-Tg mice attenuates AD-like neuropathology, reducing soluble $A\beta_{(1-42)}$ and aggregated Aβ plaques and enhancing dentate gyrus (DG) neurogenesis and cognitive performance.[39,40] To examine whether repeated GA immunization induces *Egr1* expression in AD, we first assessed EGR1 protein levels by immunohistochemistry in brain coronal cryosections.

Three experimental groups were studied: GA-immunized versus PBS-treated AD-Tg mice, in a regimen of weekly injections for 3 consecutive months starting at a symptom-onset age of 7 months, and age-matched naive non-Tg (wt) control mice. Basal levels of EGR1 immunoreactivity were observed in wt brains (Fig. 3A). Specifically in the hippocampus, EGR1 was elevated in AD-Tg mice compared with wt control mice (Fig. 3A vs. 3B). Importantly, a further increase in EGR1 immunoreactivity was observed after GA immunization of AD-Tg mice (Figs. 3B vs. 3C). High-magnification (100×) images clearly demonstrated elevated nuclear EGR1 immunoreactivity in the DG of GA-immunized compared with PBS control AD-Tg mice (Figs. 3E vs. 3D), in a pattern reminiscent of immature neurons primarily located in the subgranular zone (SGZ) and the granular cell layer (GCL; Figs. 3C, 3E). This is consistent with previous studies reporting elevated EGR1 levels in support of neurogenesis and cognition within this region.[83,86–88]

Multiple EGR1-positive cells in GA-immunized AD-Tg mice were colabeled with Ki67, a nuclear protein associated with cell proliferation, in the SGZ and GCL (Fig. 3F). We further analyzed the DG of corresponding brain section coexpression of EGR1 and double cortin (DCX), a marker for newly formed neurons. Overall, fewer DCX-positive cells containing fewer cell dendrites were observed in PBS-treated compared with GA-immunized AD-Tg mice (Fig. 3G vs. 3H). In GA-immunized but not in PBS-treated AD-Tg mice, newly formed neurons frequently coexpressed DCX and EGR1 (arrowheads; Figs. 3H–K vs. 3G). To quantify the number of EGR1-immunoreactive cells, we used an immunoperoxidase-based reaction with DAB substrate on brain sections from GA-immunized and PBS-treated mice (Figs. 3L, 3M). A significant increase of 35% in the number of cells expressing nuclear EGR1 in the DG was found in GA-immunized compared with PBS-treated AD-Tg mice (Fig. 3N; $P < 0.01$). We interpreted the high EGR1 expression in the DG, especially by proliferating neuronal cells as an indicator of tissue regeneration and a downstream result of GA immunization in AD mice.

To further validate increased EGR1 levels in the hippocampus after GA immunization, we analyzed the soluble protein extracts from nuclear fractions of the hippocampus by Western blot using EGR1-specific antibodies (Fig. 4A). We detected three protein bands (with apparent molecular masses of 82 kDa, 80 kDa, and 75 kDa) that specifically react with anti-EGR1 antibody showing similar intensities (Fig. 4A); therefore, quantification was performed collectively for all three bands. A higher EGR1 band possibly corresponding to EGR1 dimeric/oligomeric isoforms (with apparent molecular mass of 140 kDa) was also obtained, with quantitative elevation of 54% in AD control (vs. the non-Tg wt) mice and 50% elevation after GA immunization (data not shown). Quantitative Western blot analysis of the most intense bands (75–82 kDa) indicated significant alterations (Fig. 4B; $P = 0.0002$) in protein levels of nuclear EGR1 in the hippocampus under an AD-like condition (54% elevation) in the PBS-treated compared with wt mice (Fig. 4B). GA immunization significantly increased EGR1 protein levels by an additional 30% compared with PBS-treated (AD control) mice (Fig. 4B). Further examination of *Egr1* mRNA relative expression levels in the brains of the same animals, using quantitative real-time PCR analysis, showed a nonsignificant trend of increased *Egr1* levels in GA-immunized AD-Tg mice compared with nonimmunized AD-Tg mice (Fig. 4C). In the wt naive mice, levels of *Egr1* mRNA were the highest, in contrast to the lowest levels of EGR1 protein observed in the Western blot analysis (Figs. 4C vs. 4B). In the chronic AD models, unlike in the induced-glaucoma models, the elevation of *Egr1* expression was found under AD pathologic conditions in the absence of GA treatment, with treatment further boosting its levels. This may imply that EGR1 protein is consistently elevated in response to chronic AD insult as a repair mechanism and is further elevated by GA protective immunization.

Correlation analysis of *Egr1* mRNA and protein levels with two aspects of AD-like neuropathology in AD-Tg mice ($n = 14$) yielded a significant negative association between EGR1 nuclear protein in the hippocampus and total hippocampal Aβ plaque area (Figs. 4D, 4E; $P = 0.0076$). Additional correlation analyses between *Egr1* mRNA and hippocampal Aβ plaque area and soluble toxic $A\beta_{(1-42)}$ in the brain were also negative but did not reach significance (Figs. 4D, 4F).

DISCUSSION

This study identifies global gene expression alterations induced by GA-protective immunization in elevated-IOP rat retinas. Gene set analysis of GA-induced genes according to ontological classification (AmiGO) revealed the repression of ontologies associated with cell death, scar tissue formation, immune responses, and protein degradation and the induction of ontologies involved with growth and neurogenesis, cell migration and communication, and transcription regulation. Comprehensive DAVID functional annotation enrichment analysis identified multiple terms that supported these findings and further indicated other overenriched terms such as glycoprotein, ex-

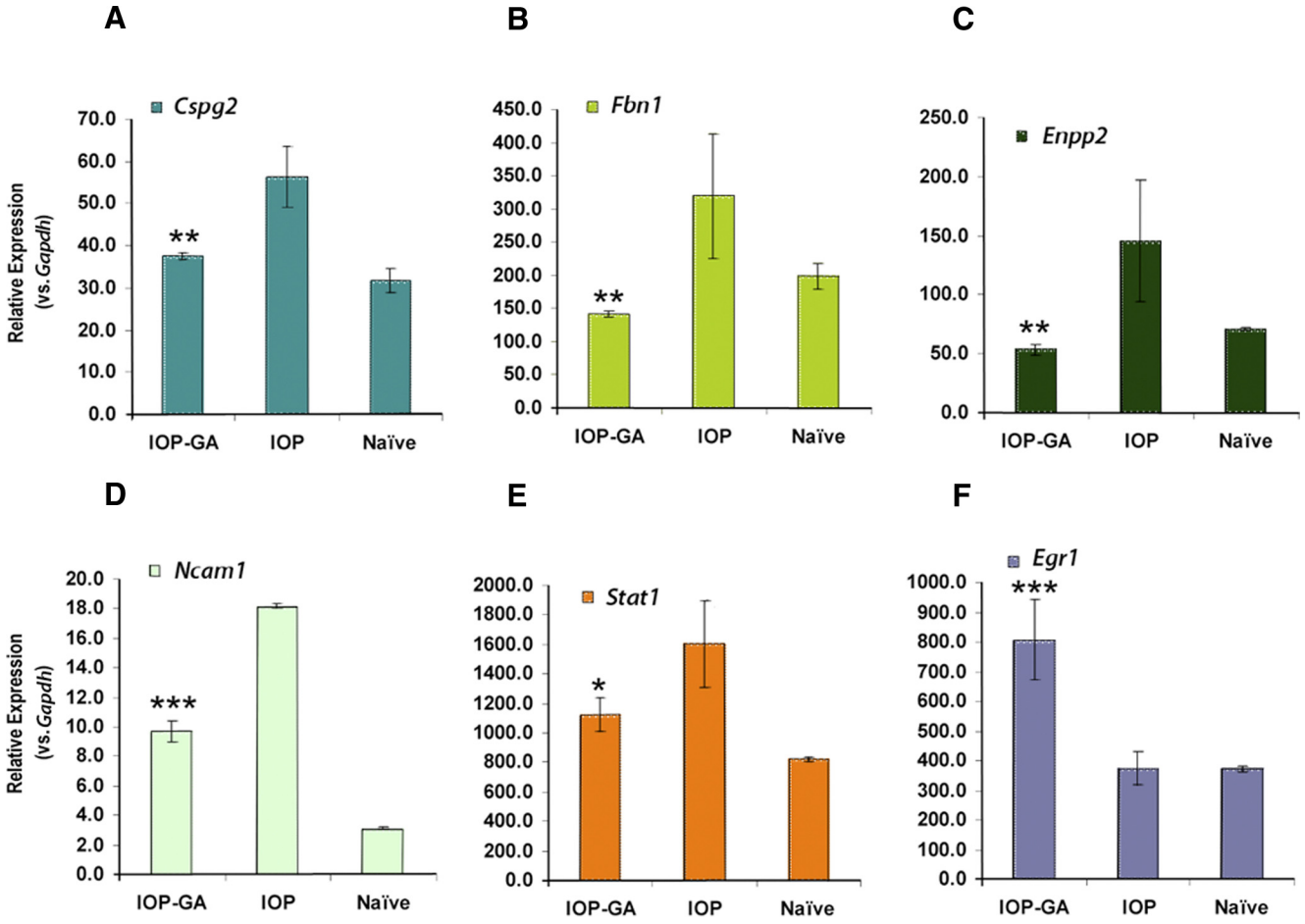

FIGURE 2. Quantitative real-time PCR analyses demonstrating gene expression profiles of a selected group of prominently altered genes after GA immunization in elevated IOP rats. (**A–F**) Ratios refer to the relative expression of genes between IOP-GA and IOP-PBS groups. Genes are compared with the *Gapdh* reference gene, and each animal was analyzed separately in triplicate. These results were validated twice also using *β-Actin* as a reference gene. (**A–E**) Graphs demonstrate genes that were induced in the retina by IOP elevation and attenuated 1 week after GA immunization, representing the category of genes restored to homeostatic levels (normal) by GA. In this category, we included genes involved in the formation of scar tissue/matrix components, lipid signaling enzyme, cell-to-cell adhesion, synaptic plasticity, and immune responses. (**F**) *Egr1*, a transcription regulator of immune-related genes, as well as synaptic plasticity and neurogenesis-associated genes, was uniquely induced by GA immunization. Error bars indicate mean ± SD (*$P < 0.01$; **$P < 0.001$; ***$P < 0.0001$, by two-tailed Student's *t*-test).

tracellular matrix formation, and synapse. KEGG pathway analysis that allows for mapping networks of molecular and cellular interactions emphasized a significantly enriched pathway of the aminoacyl-tRNA biosynthesis. This pathway was previously reported to be involved in endogenous neuroprotection provoked by ischemic preconditioning in the rat retina of a chronic glaucoma model.[77] Specifically, one of the most prominent changes in gene expression induced by GA immunization was an upregulation of the transcription factor *Egr1*, associated with cell survival, neurogenesis, and immune responses to CNS damage. Interestingly, similar changes in gene regulation of the aminoacyl-tRNA biosynthesis genes (repression of *Iars, Yars, Cars, Lars,* and *Mars*) and *Egr1* gene (induction), as observed in this study, were also obtained after neuroprotection in the glaucoma rat model.[77] *Egr1,* which is involved in learning and memory processes, was found here to be elevated in the hippocampus of AD transgenic mice after GA immunization. Hippocampal neurogenesis has been a well-established phenomenon[89–91] and was shown to be enhanced after GA immunization in AD transgenic mice.[39] These results may indicate a role for EGR1 in both neuroprotection and hippocampal neurogenesis/cognition, accounting for some of the beneficial effects of GA immunization in animal models of neurodegeneration.

The present study reveals multiple gene expression alterations in adult rat retina, induced by GA, associated with neuronal survival and plasticity, neurogenesis and immune-modulation. One week after GA immunization, gene expression profiles from elevated-IOP rat retinas revealed mostly a pattern of reduction or induction toward homeostatic or "normal" basal levels. These genes include a group of glycoproteins and matrix-adherent proteins, such as fibulin *(Fbln)1, Fbn1, Cspg2, Ncam1, Enpp2*, a disintegrin and metalloprotease domain (*Adam)10*, and lectin galactoside-binding soluble (*Lgals)5* and *3bp*. GA immunization also restored homeostasis by modulating the expression of genes associated with immune activity, including *Stat1*, tumor necrosis factor-α (*Tnf-α*), interferons *(Ifn)-α* and *(Ifn)-γ*, transforming growth factor β receptor (*Tgf-β*)1, and major histocompatibility complex *(Rt)* class I.

Genes induced or repressed specifically by GA, but not altered by elevated-IOP conditions, included transcription and neurogenesis factors, such as Smad homolog 5 (*Madh5*; 43% induction) and Smad homolog 7 (*Madh7*; 24% induction). The former affects the BMP signaling pathway,[92] and the latter acts as a common partner in SMAD protein phosphorylation (an intracellular protein that transduces extracellular signals to activate *Tgf-β* gene transcription).[93] The small but significant upregulation toward normalization of *Noggin* and the induc-

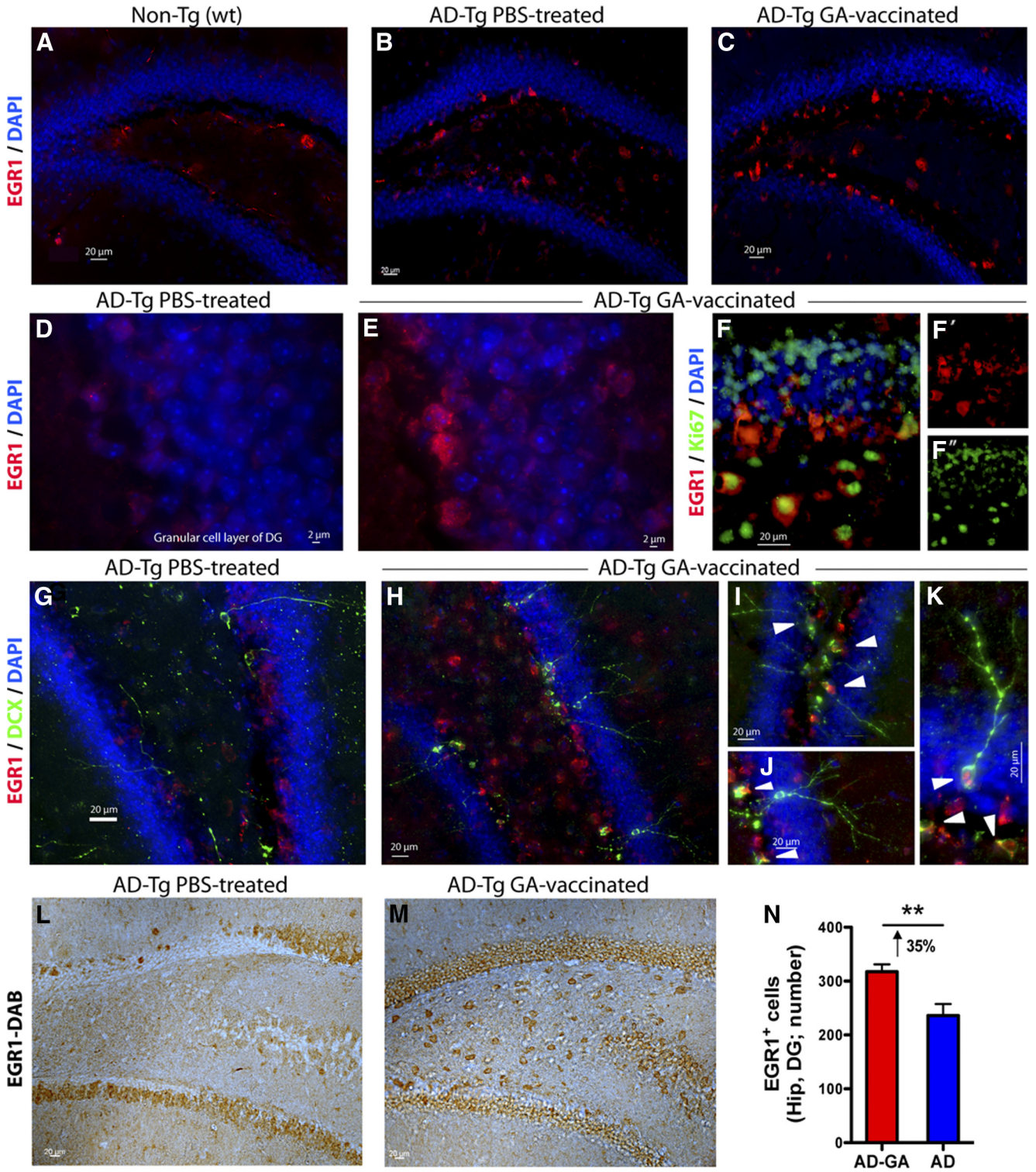

Figure 3. Enhanced hippocampal EGR1-immunoreactivity in the dentate gyrus NPCs in AD-Tg mice after GA immunization. (**A–C**) Representative images of coronal brain sections of hippocampal dentate gyrus (DG) from PBS-treated compared with GA-immunized AD-Tg mice and of age-matched wt littermates (Non-Tg), with GA-immunized mice exhibiting higher levels of EGR1-immunoreactivity in the DG. (**D**, **E**) Higher magnification images demonstrate nuclear staining of EGR1 in the subgranular zones and granular cell layers of the DG, highlighting the difference in EGR1 expression pattern between PBS- and GA-immunized mice. (**F**) Immunoreactivity of Ki-67, a nuclear marker for cell proliferation, in a GA-immunized mouse, demonstrating the colabeling of proliferating cells with EGR1. (**G–K**) Comparison between PBS- and GA-immunized mice showing EGR1 colabels with the newly formed neurons marker double cortin (DCX), in the hippocampal DG. Overall, increased numbers of DCX-positive cells were found in GA-immunized versus PBS-treated AD-Tg mice, whereas the GA-immunized mice demonstrated more cells colabeled with both DCX and EGR1. (**L**, **M**) Representative images of EGR1 detection by peroxidase-based staining (using DAB as a chromogen/substrate) in PBS- versus GA-immunized mice. (**N**) Quantitative analysis of the number of EGR1-DAB–positive cells reveals an increase of approximately 35% after GA immunization in the hippocampus of AD-Tg mice (**$P < 0.01$; by two-tailed Student's *t*-test). Results are presented as mean ± SEM from three independent experiments.

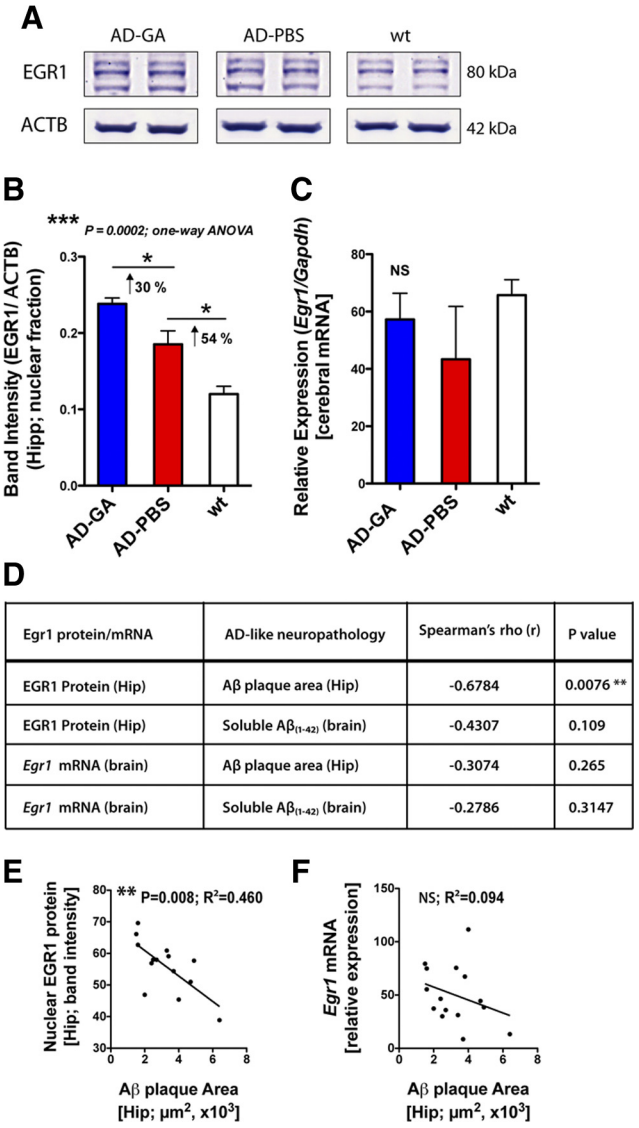

Egr1 protein/mRNA	AD-like neuropathology	Spearman's rho (r)	P value
EGR1 Protein (Hip)	Aβ plaque area (Hip)	-0.6784	0.0076 **
EGR1 Protein (Hip)	Soluble $A\beta_{(1-42)}$ (brain)	-0.4307	0.109
Egr1 mRNA (brain)	Aβ plaque area (Hip)	-0.3074	0.265
Egr1 mRNA (brain)	Soluble $A\beta_{(1-42)}$ (brain)	-0.2786	0.3147

FIGURE 4. Analysis of EGR1 protein expression in the hippocampus of AD-Tg mice following GA immunization. (**A**) Hippocampus nuclear protein fractions were prepared from Non-Tg (wt), PBS-treated, and GA-immunized AD-Tg mice, and levels of EGR1 protein were analyzed by Western blot. Representative Western blot shown ($n = 7$ per group). Blots were incubated with antibodies against total EGR1 and ACTB as a reference protein loading control. (**B**) Densitometric quantification of EGR1 levels. The graph displays the average EGR1 band densities normalized for total ACTB levels in the lysates from each testing group. Increased levels of EGR1 are observed in AD compared with wt mice, and a further significant increase is found after GA immunization ($P = 0.0002$, by one-way ANOVA and Bonferroni's multiple comparison posttest). (**C**) Quantitative real-time PCR analysis of relative mRNA expression levels of *Egr1* (vs. *Gapdh*) in brains from the same animals that were analyzed for protein levels using Western blot. Results are presented as mean ± SEM from three independent experiments. (**D**–**F**) Correlation analysis of Egr1 mRNA and protein levels with two aspects of AD-like neuropathology in AD-Tg mice ($n = 14$) yields a significant negative association between EGR1 nuclear protein in the hippocampus and the hippocampal Aβ plaque area. (**D**) Table lists pairs of correlations using a nonparametric test, with Spearman's rho (ρ) and P values. (**E**, **F**) Graphs display two representative correlation analyses between *Egr1* mRNA and protein and Aβ plaque area in the hippocampus (as in the table in **D**), where individual pair dots and R^2 values are indicated. NS, not significant. * $P < 0.05$; *** $P < 0.001$.

tion of *Madh* members including *Tgf-β1*, specifically by GA, suggest a general mechanism by which GA may promote the differentiation of neuronal progenitor cells (NPCs) to neurons rather than to glial cells in the retina and stimulate local TGF-β expression for neurotrophic support.[94,95]

In adult neurons, immediate-early genes (IEGs) such as *Egr1* are expressed both constitutively and in response to afferent activity.[83,87,88,96–99] It has been suggested that during learning, IEGs play a role in the signal cascade, resulting in the expression of downstream genes critical for the consolidation of long-term potentiation and memory.[82,100] Specifically, *Egr1* was shown to be highly involved in regulating hippocampal function through the induction of plasticity and memory reactivation.[80]

In the present study, results from microarray analyses and real-time PCR revealed that the *Egr1* nuclear transcription factor was substantially induced by GA immunization in elevated-IOP rat retinas. Although analysis of EGR1 protein was not performed in the elevated-IOP rat retina, it was already known to be expressed in cells of the inner nuclear layer and the ganglion cell layer.[101,102] Alterations in *Egr1* gene and protein levels were also correlated with RGC loss.[103–105] EGR1 was implicated in retinal development, interconnectivity between small and large RGCs, and activity dysfunction.[102,106] Moreover, retinal neuroprotection and axonal sprouting were shown to coincide with elevated *Egr1* levels in ischemic and optic nerve lesion animal models.[107,108] In the brain, *Egr* family of transcription factors has been implicated in rapid regulation of gene expression that underlies neuronal plasticity.[100,109] In a transgenic APP751SL mouse model of AD, EGR1 immunoreactivity in the CA1 region of the hippocampus increased in response to short-term and long-term memory tasks.[110] EGR1 protein was further suggested to play a role in orchestrating neuronal network restructuring in response to an enriched environment.[111]

In AD-Tg mice, GA immunization significantly increased levels of EGR1, as assessed by both quantitative immunohistochemistry of EGR1-positive cells in the DG and by Western blot of nuclear EGR1 protein in the hippocampus. EGR1 levels were elevated in the disease condition and further increased after immunization. This increase was still apparent 1 month after the last GA administration, occurring most notably in proliferating Ki67-positive and DCX-positive newly formed hippocampal neurons. Protein analysis by Western blot, showing products of various size as previously reported by others,[112–115] suggested that EGR1 may undergo posttranslational modifications to differentially regulate downstream genes. It is possible that EGR1 forms a multimeric complex with other transcription factors to finely modulate important cellular responses. In that case, the more subtle changes of EGR1 by long-term GA treatment in the chronic AD model (0.3-fold by protein; NS elevation trend in the transcript levels) versus the immediate response to GA in the glaucoma model (twofold by transcript) may speak to the time-dependent mechanism by which GA immunization provides benefit and may translate to greater effects on CNS repair.

Interestingly, the negative correlation that we found between nuclear EGR1 protein and Aβ plaque burden in the hippocampus of AD-Tg mice implies that these factors are associated and possibly influence each other. We found relatively high proportions ($R^2 = 0.46$) of the variability in Aβ plaques that may be explained by variation in EGR1 nuclear protein in the hippocampus. It is possible that higher levels of EGR1 were a result of GA effects on reduced Aβ plaques and soluble toxic $A\beta_{(1-42)}$ or that EGR1 directly contributed to their reduction in the hippocampus. Future studies are warranted to explore the possible role of EGR1 in AD repair.

In response to stress signals such as CNS insult, EGR1 is rapidly elevated and regulates the expression of multiple downstream genes.[79] Many of these genes are associated with neuronal potentiation, plasticity, neurogenesis, memory, and learning.[80,116] In agreement with results from this study, recent reports[110,117] using alternative mouse models of AD demonstrated that EGR1-induced hippocampal neurogenesis and neuronal function correlate with benefits from effective immunotherapy and that spatial memory deficits are associated with hippocampal impairment of learning-induced EGR1 activation. The present data may explain our previous observations of GA-induced hippocampal DG neurogenesis that could, at least in part, be a result of enhanced levels of EGR1.[39]

Previous studies[26,39] from our group, after GA or similar T cell-based immunization of AD mice, documented a local shift toward a helper T cell type 2 (Th2) cytokine profile with an increase in the Th2-derived cytokine interleukin (IL)-4. We have also shown that microglia/macrophages activated by IL-4 are capable of overcoming Aβ-induced neurotoxicity, supporting cell survival and neurogenesis in vitro.[39,118,119] In this context, a recent study reporting that EGR1 specifically binds to the IL-4 gene promoter and stimulates its transcription,[120] could provide a link to GA-induced neuroprotection.

The global mechanisms by which GA immunization brings about CNS repair are still a matter of debate. In the present study, we identified multiple genes that were differentially expressed after GA treatment, thereby identifying some neuroprotective key players. Specifically, the fact that Egr1 was significantly elevated by GA treatment in both neurodegenerative models suggests that this gene and its downstream targets may play a key role in mediating a common immune-related protective response. It is possible that Egr1 induction after GA immunization is a direct result of the increased recruitment of beneficial T cells and monocytes to the CNS with a local shift in the immune-molecular milieu[19,26,39,40] or that it is an indirect reflection of a healthier, less toxic tissue, associated with repair. As a transcription factor affecting multiple downstream genes found to be enriched in various pathways, EGR1 is likely to be involved in the GA-mediated prevention of RGC death and the attenuation of functional decline in glaucoma.[38,48] In the context of AD, EGR1 may be implicated in GA-mediated enhanced capacity for regeneration in the DG and improved cognition.[39] Further research is needed to elucidate the possible role of EGR1 in immunomodulation, neuroprotection, and regeneration in the diseased CNS.

Acknowledgments

The authors thank Michal Schwartz (The Weizmann Institute of Science, Israel) for scientific advice and support and Gideon Rechavi, Jasmine Jacob, and Ron Ophir for their contribution to the Affymetrix microarrays and statistical analysis.

References

1. Arundine M, Tymianski M. Molecular mechanisms of glutamate-dependent neurodegeneration in ischemia and traumatic brain injury. *Cell Mol Life Sci.* 2004;61:657–668.
2. Butterfield DA, Boyd-Kimball D. Amyloid beta-peptide(1–42) contributes to the oxidative stress and neurodegeneration found in Alzheimer disease brain. *Brain Pathol.* 2004;14:426–432.
3. Dawson VL, Dawson TM. Nitric oxide in neurodegeneration. *Prog Brain Res.* 1998;118:215–229.
4. Driscoll M, Gerstbrein B. Dying for a cause: invertebrate genetics takes on human neurodegeneration. *Nat Rev Genet.* 2003;4:181–194.
5. Hoyer S. Neurodegeneration, Alzheimer's disease, and beta-amyloid toxicity. *Life Sci.* 1994;55:1977–1983.
6. Kawahara M, Kuroda Y. Molecular mechanism of neurodegeneration induced by Alzheimer's beta-amyloid protein: channel formation and disruption of calcium homeostasis. *Brain Res Bull.* 2000;53:389–397.
7. Moncada S, Bolanos JP. Nitric oxide, cell bioenergetics and neurodegeneration. *J Neurochem.* 2006;97:1676–1689.
8. Paulson HL. Toward an understanding of polyglutamine neurodegeneration. *Brain Pathol.* 2000;10:293–299.
9. Eikelenboom P, Bate C, Van Gool WA, et al. Neuroinflammation in Alzheimer's disease and prion disease. *Glia.* 2002;40:232–239.
10. Harry GJ, Kraft AD. Neuroinflammation and microglia: considerations and approaches for neurotoxicity assessment. *Expert Opin Drug Metab Toxicol.* 2008;4:1265–1277.
11. Lehnardt S. Innate immunity and neuroinflammation in the CNS: the role of microglia in Toll-like receptor-mediated neuronal injury. *Glia*. 58:253–263.
12. Mueller FJ, McKercher SR, Imitola J, et al. At the interface of the immune system and the nervous system: how neuroinflammation modulates the fate of neural progenitors in vivo. *Ernst Schering Res Found Workshop.* 2005;83–114.
13. Ray B, Lahiri DK. Neuroinflammation in Alzheimer's disease: different molecular targets and potential therapeutic agents including curcumin. *Curr Opin Pharmacol.* 2009;9:434–444.
14. Rojo LE, Fernandez JA, Maccioni AA, Jimenez JM, Maccioni RB. Neuroinflammation: implications for the pathogenesis and molecular diagnosis of Alzheimer's disease. *Arch Med Res.* 2008;39:1–16.
15. Sparkman NL, Johnson RW. Neuroinflammation associated with aging sensitizes the brain to the effects of infection or stress. *Neuroimmunomodulation.* 2008;15:323–330.
16. Tansey MG, Goldberg MS. Neuroinflammation in Parkinson's disease: its role in neuronal death and implications for therapeutic intervention. *Neurobiol Dis*. 37:510–518.
17. Vesce S, Rossi D, Brambilla L, Volterra A. Glutamate release from astrocytes in physiological conditions and in neurodegenerative disorders characterized by neuroinflammation. *Int Rev Neurobiol.* 2007;82:57–71.
18. Avidan H, Kipnis J, Butovsky O, Caspi RR, Schwartz M. Vaccination with autoantigen protects against aggregated beta-amyloid and glutamate toxicity by controlling microglia: effect of CD4+CD25+ T cells. *Eur J Immunol.* 2004;34:3434–3445.
19. Bakalash S, Shlomo GB, Aloni E, et al. T-cell-based vaccination for morphological and functional neuroprotection in a rat model of chronically elevated intraocular pressure. *J Mol Med.* 2005;83:904–916.
20. Barouch R, Schwartz M. Autoreactive T cells induce neurotrophin production by immune and neural cells in injured rat optic nerve: implications for protective autoimmunity. *FASEB J.* 2002;16:1304–1306.
21. Cohen IR, Schwartz M. Autoimmune maintenance and neuroprotection of the central nervous system. *J Neuroimmunol.* 1999;100:111–114.
22. Fisher J, Levkovitch-Verbin H, Schori H, et al. Vaccination for neuroprotection in the mouse optic nerve: implications for optic neuropathies. *J Neurosci.* 2001;21:136–142.
23. Frenkel D, Huang Z, Maron R, Koldzic DN, Moskowitz MA, Weiner HL. Neuroprotection by IL-10-producing MOG CD4+ T cells following ischemic stroke. *J Neurol Sci.* 2005;233:125–132.
24. Kipnis J, Mizrahi T, Yoles E, Ben-Nun A, Schwartz M. Myelin specific Th1 cells are necessary for post-traumatic protective autoimmunity. *J Neuroimmunol.* 2002;130:78–85.
25. Kipnis J, Schwartz M. Controlled autoimmunity in CNS maintenance and repair: naturally occurring CD4+CD25+ regulatory T-Cells at the crossroads of health and disease. *Neuromolecular Med.* 2005;7:197–206.
26. Koronyo-Hamaoui M, Ko MK, Koronyo Y, et al. Attenuation of AD-like neuropathology by harnessing peripheral immune cells: local elevation of IL-10 and MMP-9. *J Neurochem.* 2009;111:1409–1424.
27. Moalem G, Leibowitz-Amit R, Yoles E, Mor F, Cohen IR, Schwartz M. Autoimmune T cells protect neurons from secondary degeneration after central nervous system axotomy. *Nat Med.* 1999;5:49–55.
28. Monsonego A, Beserman ZP, Kipnis J, Yoles E, Weiner HL, Schwartz M. Beneficial effect of orally administered myelin basic

protein in EAE-susceptible Lewis rats in a model of acute CNS degeneration. *J Autoimmun.* 2003;21:131–138.
29. Ron-Harel N, Schwartz M. Immune senescence and brain aging: can rejuvenation of immunity reverse memory loss? *Trends Neurosci.* 2009;32:367–375.
30. Schori H, Yoles E, Schwartz M. T-cell-based immunity counteracts the potential toxicity of glutamate in the central nervous system. *J Neuroimmunol.* 2001;119:199–204.
31. Schwartz M, London A, Shechter R. Boosting T-cell immunity as a therapeutic approach for neurodegenerative conditions: the role of innate immunity. *Neuroscience.* 2009;158:1133–1142.
32. Schwartz M, Moalem G. Beneficial immune activity after CNS injury: prospects for vaccination. *J Neuroimmunol.* 2001;113: 185–192.
33. Schwartz M, Shechter R. Systemic inflammatory cells fight off neurodegenerative disease. *Nat Rev Neurol*. 2010;6:405–410.
34. Ziv Y, Ron N, Butovsky O, et al. Immune cells contribute to the maintenance of neurogenesis and spatial learning abilities in adulthood. *Nat Neurosci.* 2006;9:268–275.
35. Teitelbaum D, Arnon R, Sela M. Cop 1 as a candidate drug for multiple sclerosis. *J Neural Transm Suppl.* 1997;49:85–91.
36. Teitelbaum D, Aharoni R, Arnon R, Sela M. Specific inhibition of the T-cell response to myelin basic protein by the synthetic copolymer Cop 1. *Proc Natl Acad Sci U S A.* 1988;85:9724–9728.
37. Bakalash S, Kessler A, Mizrahi T, Nussenblatt R, Schwartz M. Antigenic specificity of immunoprotective therapeutic vaccination for glaucoma. *Invest Ophthalmol Vis Sci.* 2003;44:3374–3381.
38. Bakalash S, Kipnis J, Yoles E, Schwartz M. Resistance of retinal ganglion cells to an increase in intraocular pressure is immune-dependent. *Invest Ophthalmol Vis Sci.* 2002;43:2648–2653.
39. Butovsky O, Koronyo-Hamaoui M, Kunis G, et al. Glatiramer acetate fights against Alzheimer's disease by inducing dendritic-like microglia expressing insulin-like growth factor 1. *Proc Natl Acad Sci U S A.* 2006;103:11784–11789.
40. Butovsky O, Kunis G, Koronyo-Hamaoui M, Schwartz M. Selective ablation of bone marrow-derived dendritic cells increases amyloid plaques in a mouse Alzheimer's disease model. *Eur J Neurosci.* 2007;26:413–416.
41. Frenkel D, Maron R, Burt DS, Weiner HL. Nasal vaccination with a proteosome-based adjuvant and glatiramer acetate clears beta-amyloid in a mouse model of Alzheimer disease. *J Clin Invest.* 2005;115:2423–2433.
42. Kipnis J, Schwartz M. Dual action of glatiramer acetate (Cop-1) in the treatment of CNS autoimmune and neurodegenerative disorders. *Trends Mol Med.* 2002;8:319–323.
43. Kipnis J, Yoles E, Porat Z, et al. T cell immunity to copolymer 1 confers neuroprotection on the damaged optic nerve: possible therapy for optic neuropathies. *Proc Natl Acad Sci U S A.* 2000; 97:7446–7451.
44. Shechter R, London A, Varol C, et al. Infiltrating blood-derived macrophages are vital cells playing an anti-inflammatory role in recovery from spinal cord injury in mice. *PLoS Med.* 2009;6: e1000113.
45. Salumbides B, Koronyo Y, Pham M, et al. Immune-based combination therapy reduces Alzheimer's Disease pathology in preclinical models (Abstract). *J Neurosci*. 2010;(suppl): 556.
46. WoldeMussie E, Ruiz G, Wijono M, Wheeler LA. Neuroprotection of retinal ganglion cells by brimonidine in rats with laser-induced chronic ocular hypertension. *Invest Ophthalmol Vis Sci.* 2001; 42:2849–2855.
47. Levkovitch-Verbin H. Animal models of optic nerve diseases. *Eye (Lond).* 2004;18:1066–1074.
48. Ben-Shlomo G, Bakalash S, Lambrou GN, et al. Pattern electroretinography in a rat model of ocular hypertension: functional evidence for early detection of inner retinal damage. *Exp Eye Res.* 2005;81:340–349.
49. Bayer AU, Ferrari F. Severe progression of glaucomatous optic neuropathy in patients with Alzheimer's disease. *Eye (Lond).* 2002;16:209–212.
50. Bayer AU, Ferrari F, Erb C. High occurrence rate of glaucoma among patients with Alzheimer's disease. *Eur Neurol.* 2002;47: 165–168.
51. Bayer AU, Keller ON, Ferrari F, Maag KP. Association of glaucoma with neurodegenerative diseases with apoptotic cell death: Alzheimer's disease and Parkinson's disease. *Am J Ophthalmol.* 2002;133:135–137.
52. Guo L, Duggan J, Cordeiro MF. Alzheimer's disease and retinal neurodegeneration. *Curr Alzheimer Res*. 2010;7:3–14.
53. Guo L, Salt TE, Luong V, et al. Targeting amyloid-beta in glaucoma treatment. *Proc Natl Acad Sci U S A.* 2007;104:13444–13449.
54. Karseras AG. Progressive glaucoma in patients with Alzheimer's disease. *Eye (Lond).* 2004;18:229.
55. Koronyo-Hamaoui M, Koronyo Y, Ljubimov AV, et al. Identification of amyloid plaques in retinas from Alzheimer's patients and noninvasive in vivo optical imaging of retinal plaques in a mouse model. *Neuroimage*. 54(suppl 1):S204–S217.
56. McKinnon SJ. Glaucoma: ocular Alzheimer's disease? *Front Biosci.* 2003;8:s1140–s1156.
57. Parisi V. Correlation between morphological and functional retinal impairment in patients affected by ocular hypertension, glaucoma, demyelinating optic neuritis and Alzheimer's disease. *Semin Ophthalmol.* 2003;18:50–57.
58. Tamura H, Kawakami H, Kanamoto T, et al. High frequency of open-angle glaucoma in Japanese patients with Alzheimer's disease. *J Neurol Sci.* 2006;246:79–83.
59. Tsuruma K, Tanaka Y, Shimazawa M, Hara H. Induction of amyloid precursor protein by the neurotoxic peptide, amyloid-beta 25–35, causes retinal ganglion cell death. *J Neurochem*. 2010; 113:1545–1554.
60. Wostyn P, Audenaert K, De Deyn PP. Alzheimer's disease: cerebral glaucoma? *Med Hypotheses*. 74:973–977.
61. Wostyn P, Audenaert K, De Deyn PP. Alzheimer's disease and glaucoma: is there a causal relationship? *Br J Ophthalmol.* 2009; 93:1557–1559.
62. Vickers JC. The cellular mechanism underlying neuronal degeneration in glaucoma: parallels with Alzheimer's disease. *Aust N Z J Ophthalmol.* 1997;25:105–109.
63. Yin H, Chen L, Chen X, Liu X. Soluble amyloid beta oligomers may contribute to apoptosis of retinal ganglion cells in glaucoma. *Med Hypotheses.* 2008;71:77–80.
64. Yoneda S, Hara H, Hirata A, Fukushima M, Inomata Y, Tanihara H. Vitreous fluid levels of beta-amyloid((1–42)) and tau in patients with retinal diseases. *Jpn J Ophthalmol.* 2005;49:106–108.
65. Schwartz M, Kipnis J. Therapeutic T cell-based vaccination for neurodegenerative disorders: the role of CD4+CD25+ regulatory T cells. *Ann N Y Acad Sci.* 2005;1051:701–708.
66. Weber MS, Prod'homme T, Youssef S, et al. Type II monocytes modulate T cell-mediated central nervous system autoimmune disease. *Nat Med.* 2007;13:935–943.
67. Jankowsky JL, Fadale DJ, Anderson J, et al. Mutant presenilins specifically elevate the levels of the 42 residue beta-amyloid peptide in vivo: evidence for augmentation of a 42-specific gamma secretase. *Hum Mol Genet.* 2004;13:159–170.
68. Schori H, Kipnis J, Yoles E, et al. Vaccination for protection of retinal ganglion cells against death from glutamate cytotoxicity and ocular hypertension: implications for glaucoma. *Proc Natl Acad Sci U S A.* 2001;98:3398–3403.
69. Levkovitch-Verbin H, Quigley HA, Martin KR, Valenta D, Baumrind LA, Pease ME. Translimbal laser photocoagulation to the trabecular meshwork as a model of glaucoma in rats. *Invest Ophthalmol Vis Sci.* 2002;43:402–410.
70. Jia L, Cepurna WO, Johnson EC, Morrison JC. Patterns of intraocular pressure elevation after aqueous humor outflow obstruction in rats. *Invest Ophthalmol Vis Sci.* 2000;41:1380–1385.
71. Irizarry RA, Hobbs B, Collin F, et al. Exploration, normalization, and summaries of high density oligonucleotide array probe level data. *Biostatistics.* 2003;4:249–264.
72. Gentleman RC, Carey VJ, Bates DM, et al. Bioconductor: open software development for computational biology and bioinformatics. *Genome Biol.* 2004;5:R80.
73. Smyth GK. Linear models and empirical bayes methods for assessing differential expression in microarray experiments. *Stat Appl Genet Mol Biol.* 2004;3:Article3.

74. Huang da W, Sherman BT, Lempicki RA. Systematic and integrative analysis of large gene lists using DAVID bioinformatics resources. *Nat Protoc.* 2009;4:44–57.
75. Huang da W, Sherman BT, Lempicki RA. Bioinformatics enrichment tools: paths toward the comprehensive functional analysis of large gene lists. *Nucleic Acids Res.* 2009;37:1–13.
76. Livak KJ, Schmittgen TD. Analysis of relative gene expression data using real-time quantitative PCR and the 2(-Delta Delta C(T)) Method. *Methods.* 2001;25:402–408.
77. Kamphuis W, Dijk F, van Soest S, Bergen AA. Global gene expression profiling of ischemic preconditioning in the rat retina. *Mol Vis.* 2007;13:1020–1030.
78. Gomez-Martin D, Diaz-Zamudio M, Galindo-Campos M, Alcocer-Varela J. Early growth response transcription factors and the modulation of immune response: implications towards autoimmunity. *Autoimmun Rev.* 2010;9:454–458.
79. O'Donovan KJ, Tourtellotte WG, Millbrandt J, Baraban JM. The EGR family of transcription-regulatory factors: progress at the interface of molecular and systems neuroscience. *Trends Neurosci.* 1999;22:167–173.
80. Renbaum P, Beeri R, Gabai E, et al. Egr-1 upregulates the Alzheimer's disease presenilin-2 gene in neuronal cells. *Gene.* 2003;318:113–124.
81. Beckmann AM, Wilce PA. Egr transcription factors in the nervous system. *Neurochem Int.* 1997;31:477–510; discussion 517–476.
82. Jones MW, Errington ML, French PJ, et al. A requirement for the immediate early gene Zif268 in the expression of late LTP and long-term memories. *Nat Neurosci.* 2001;4:289–296.
83. Jessberger S, Kempermann G. Adult-born hippocampal neurons mature into activity-dependent responsiveness. *Eur J Neurosci.* 2003;18:2707–2712.
84. Tashiro A, Makino H, Gage FH. Experience-specific functional modification of the dentate gyrus through adult neurogenesis: a critical period during an immature stage. *J Neurosci.* 2007;27:3252–3259.
85. Bossers K, Wirz KT, Meerhoff GF, et al. Concerted changes in transcripts in the prefrontal cortex precede neuropathology in Alzheimer's disease. *Brain.* 2010;133:3699–3723.
86. Beckmann AM, Davidson MS, Goodenough S, Wilce PA. Differential expression of Egr-1-like DNA-binding activities in the naive rat brain and after excitatory stimulation. *J Neurochem.* 1997;69:2227–2237.
87. Cole AJ, Saffen DW, Baraban JM, Worley PF. Rapid increase of an immediate early gene messenger RNA in hippocampal neurons by synaptic NMDA receptor activation. *Nature.* 1989;340:474–476.
88. Farioli-Vecchioli S, Saraulli D, Costanzi M, et al. The timing of differentiation of adult hippocampal neurons is crucial for spatial memory. *PLoS Biol.* 2008;6:e246.
89. Eriksson PS, Perfilieva E, Bjork-Eriksson T, et al. Neurogenesis in the adult human hippocampus. *Nat Med.* 1998;4:1313–1317.
90. van Praag H, Schinder AF, Christie BR, Toni N, Palmer TD, Gage FH. Functional neurogenesis in the adult hippocampus. *Nature.* 2002;415:1030–1034.
91. Thuret S, Toni N, Aigner S, Yeo GW, Gage FH. Hippocampus-dependent learning is associated with adult neurogenesis in MRL/MpJ mice. *Hippocampus.* 2009;19:658–669.
92. Retting KN, Song B, Yoon BS, Lyons KM. BMP canonical Smad signaling through Smad1 and Smad5 is required for endochondral bone formation. *Development.* 2009;136:1093–1104.
93. Yan X, Liu Z, Chen Y. Regulation of TGF-beta signaling by Smad7. *Acta Biochim Biophys Sin (Shanghai).* 2009;41:263–272.
94. Wyss-Coray T. TGF-β pathway as a potential target in neurodegeneration and Alzheimer's. *Curr Alzheimer Res.* 2006;3:191–195.
95. Wyss-Coray T, Lin C, Yan F, et al. TGF-beta1 promotes microglial amyloid-beta clearance and reduces plaque burden in transgenic mice. *Nat Med.* 2001;7:612–618.
96. Lemaire P, Revelant O, Bravo R, Charnay P. Two mouse genes encoding potential transcription factors with identical DNA-binding domains are activated by growth factors in cultured cells. *Proc Natl Acad Sci U S A.* 1988;85:4691–4695.
97. Lam BY, Zhang W, Enticknap N, Haggis E, Cader MZ, Chawla S. Inverse regulation of plasticity-related immediate early genes by calcineurin in hippocampal neurons. *J Biol Chem.* 2009;284:12562–12571.
98. Murphy TH, Worley PF, Nakabeppu Y, Christy B, Gastel J, Baraban JM. Synaptic regulation of immediate early gene expression in primary cultures of cortical neurons. *J Neurochem.* 1991;57:1862–1872.
99. Yamagata K, Kaufmann WE, Lanahan A, et al. Egr3/Pilot, a zinc finger transcription factor, is rapidly regulated by activity in brain neurons and colocalizes with Egr1/zif268. *Learn Mem.* 1994;1:140–152.
100. McKee SC, Thompson CS, Sabourin LA, Hakim AM. Regulation of expression of early growth response transcription factors in rat primary cortical neurons by extracellular ATP. *Brain Res.* 2006;1088:1–11.
101. Man PS, Evans T, Carter DA. Rhythmic expression of an egr-1 transgene in rats distinguishes two populations of photoreceptor cells in the retinal outer nuclear layer. *Mol Vis.* 2008;14:1176–1186.
102. Schippert R, Burkhardt E, Feldkaemper M, Schaeffel F. Relative axial myopia in Egr-1 (ZENK) knockout mice. *Invest Ophthalmol Vis Sci.* 2007;48:11–17.
103. Ganapathy PS, Moister B, Roon P, et al. Endogenous elevation of homocysteine induces retinal neuron death in the cystathionine-beta-synthase mutant mouse. *Invest Ophthalmol Vis Sci.* 2009;50:4460–4470.
104. Bitzer M, Schaeffel F. Effects of quisqualic acid on retinal ZENK expression induced by imposed defocus in the chick eye. *Optom Vis Sci.* 2004;81:127–136.
105. Ahmed F, Brown KM, Stephan DA, Morrison JC, Johnson EC, Tomarev SI. Microarray analysis of changes in mRNA levels in the rat retina after experimental elevation of intraocular pressure. *Invest Ophthalmol Vis Sci.* 2004;45:1247–1258.
106. Ivanov D, Dvoriantchikova G, Barakat DJ, Nathanson L, Shestopalov VI. Differential gene expression profiling of large and small retinal ganglion cells. *J Neurosci Methods.* 2008;174:10–17.
107. Kamphuis W, Dijk F, Bergen AA. Ischemic preconditioning alters the pattern of gene expression changes in response to full retinal ischemia. *Mol Vis.* 2007;13:1892–1901.
108. Herdegen T, Bastmeyer M, Bahr M, Stuermer C, Bravo R, Zimmermann M. Expression of JUN, KROX, and CREB transcription factors in goldfish and rat retinal ganglion cells following optic nerve lesion is related to axonal sprouting. *J Neurobiol.* 1993;24:528–543.
109. Avey MT, Phillmore LS, MacDougall-Shackleton SA. Immediate early gene expression following exposure to acoustic and visual components of courtship in zebra finches. *Behav Brain Res.* 2005;165:247–253.
110. Blanchard J, Decorte L, Nogues X, Micheau J. Characterization of cognition alteration across the course of the disease in APP751SL mice with parallel estimation of cerebral Abeta deposition. *Behav Brain Res.* 2009;201:147–157.
111. Pinaud R. Experience-dependent immediate early gene expression in the adult central nervous system: evidence from enriched-environment studies. *Int J Neurosci.* 2004;114:321–333.
112. Hou X, Arvisais EW, Jiang C, et al. Prostaglandin F2alpha stimulates the expression and secretion of transforming growth factor B1 via induction of the early growth response 1 gene (EGR1) in the bovine corpus luteum. *Mol Endocrinol.* 2008;22:403–414.
113. Lee KH, Kim JR. Hepatocyte growth factor induced up-regulations of VEGF through Egr-1 in hepatocellular carcinoma cells. *Clin Exp Metastasis.* 2009;26:685–692.
114. Mahalingam D, Natoni A, Keane M, Samali A, Szegezdi E. Early growth response-1 is a regulator of DR5-induced apoptosis in colon cancer cells. *Br J Cancer.* 102:754–764.
115. Shin SY, Bahk YY, Ko J, et al. Suppression of Egr-1 transcription through targeting of the serum response factor by oncogenic H-Ras. *EMBO J.* 2006;25:1093–1103.
116. Abraham WC, Dragunow M, Tate WP. The role of immediate early genes in the stabilization of long-term potentiation. *Mol Neurobiol.* 1991;5:297–314.

117. Becker M, Lavie V, Solomon B. Stimulation of endogenous neurogenesis by anti-EFRH immunization in a transgenic mouse model of Alzheimer's disease. *Proc Natl Acad Sci U S A.* 2007; 104:1691–1696.

118. Butovsky O, Talpalar AE, Ben-Yaakov K, Schwartz M. Activation of microglia by aggregated beta-amyloid or lipopolysaccharide impairs MHC-II expression and renders them cytotoxic whereas IFN-gamma and IL-4 render them protective. *Mol Cell Neurosci.* 2005;29:381–393.

119. Butovsky O, Ziv Y, Schwartz A, et al. Microglia activated by IL-4 or IFN-gamma differentially induce neurogenesis and oligodendrogenesis from adult stem/progenitor cells. *Mol Cell Neurosci.* 2006;31:149–160.

120. Lohoff M, Giaisi M, Kohler R, Casper B, Krammer PH, Li-Weber M. Early growth response protein-1 (Egr-1) is preferentially expressed in T helper type 2 (Th2) cells and is involved in acute transcription of the Th2 cytokine interleukin-4. J Biol Chem 285:1643–1652.